J Electr Eng Technol.2018; 13(3): 1285-1293
http://doi.org/10.5370/JEET.2018.13.3.1285

ISSN(Print) 1975-0102
ISSN(Online) 2093-7423

A New Type of CPPM Machine with Stator Axial Magnetic Ring

Kun Xie*, **, Xinhua Li†, Jimin Ma*, Xiaojiang Wu***, Hong Yi* and Gangyi Hu****

Abstract – This paper proposes a new type of consequent-pole permanent-magnet (CPPM) machine with stator axial magnetic ring that increases torque capability over a wide speed range and enhances efficiency for the built-in rare-earth permanent magnet synchronous machine used in new energy vehicles. The excitation winding of the CPPM hybrid excitation synchronous machine in the stator is replaced by ferrite magnetic ring to simplify the structure and manufacturing process of the machine. The basic structure and magnetic regulation principle of the proposed machine are introduced and compared with the traditional interior rare-earth permanent magnet synchronous machine and CPPM hybrid excitation synchronous machine. Finally, experimental results of a new type of CPPM synchronous motor prototype with axial magnetic ring are introduced in the paper.

Keywords: Stator axial magnetic ring, CPPM synchronous machine, Magnetic regulation principle, Performance comparison, Experimental results.

1. Introduction

In recent years, interior permanent-magnet synchronous motors (IPMSMs) with Nd–Fe–B PMs are widely used in new energy vehicles due to their high efficiency and high power density [1-4]. With the growing demand for high speed drive in the application of new energy vehicles, higher requirements are put forward to the flux weakening ability in IPMSMs. However, due to the existence of the high direct axis magnetic resistance of the rare earth permanent magnet in IPMSMs, larger armature current is needed to achieve flux weakening control, than the copper loss will increase and the permanent magnet will face the demagnetization risk. Even worse, the air gap magnetic field waveform will also deteriorate, this will lead the greater iron loss under the high speed operating condition, motor temperature rise will be further increased and thus reduces motor efficiency.

So, how to broaden the flux weakening range of the IPMSMs used in the new energy vehicles is an important research topic [5~7]. Consequent-pole permanent-magnet (CPPM) machine has aroused people's attention. In [8], brushless hybrid excitation synchronous motors with improved rotors has been investigated to resolve the identified problems and improve performance. A 100 kW hybrid excitation synchronous machine drive system with the proposed control strategy is developed, experimentally realised, and validated in [9]. Prof. T.A. Lipo also developed systematic research in the CPPM axial magnetic field generator, especially in the CPPM motor design method [10, 11].

CPPM Hybrid Excitation Synchronous Motor is a synchronous motor with bidirectional magnetic adjustment. Compared with other hybrid excitation synchronous motors, the advantage of CPPM hybrid excitation synchronous motor is that the iron pole has been introduced into the rotor structure. Excitation magnetic resistance and current is small, the flux weakening range could be wide, and the DC field winding is on the stator side, eliminating the brush and slip ring, with the advantages of high reliability. However, CPPM hybrid excitation synchronous motor also has some problems, Firstly, the stator core embedded in the middle of the DC excitation winding, the installation process is complex, will also produce excitation losses, affecting the motor efficiency. Secondly, in the flux weakening speed control conditions, the axial magnetic circuit is prone to saturation, which will reduce the field weakening range. Thirdly, in the controller need to increase the DC excitation circuit will be added in the controller, which will increase the controller cost.

Aiming at the problems of permanent magnet synchronous motor and CPPM hybrid excitation synchronous motor used in new energy vehicles [12, 13]. The author proposes a new type of CPPM synchronous motor with axial magnetic ring. Compared with permanent magnet synchronous motor, CPPM synchronous motor has less direct axis magnetic circuit resistance, higher armature current regulation ability, and no permanent magnet demagnetization risk. Compared with the CPPM hybrid excitation synchronous motor, the CPPM synchronous motor replaces the excitation winding of the stator side

† Corresponding Author: School of Electrical & Electronic Engineering, Hubei University of Technology, Wuhan, 430068, China. (xhli59@163.com)
* State Key Laboratory of Ocean Engineering, Shanghai Jiao Tong University, Shanghai 200240 China. (nukeix@qq.com)
** China Ship Development and Design Center, Wuhan, Hubei 430064 China.
*** School of Electrical & Electronic Engineering, Hubei University of Technology, Wuhan, 430068, China. (yuwen026@sina.com)
Received: August 12, 2017; Accepted: January 26, 2018

with the magnetic ring, the magnetic induction shell could be omitted, the structure and the manufacturing process of the motor are simplified. Therefore, CPPM synchronous motor has a good application prospect in new energy vehicles, ships and high speed generators.

2. Basic Structure and Magnetic Modulation Principle

2.1 Basic structure

CPPM synchronous motor has the same rotor structure with the CPPM hybrid excitation synchronous motor. As shown in Fig. 1(a), CPPM synchronous motor stator permanent magnet ring has been made of ferrite permanent magnet material (Y30), axial magnetization, but eliminates the magnetic shell compared with the CPPM hybrid excitation synchronous motor. Steel sheets (50ww350) were adopted for the rotor and stator core. NdFeB permanent magnets used in rotor is N35UH (radial magnetization). The main difference in stator structure of the CPPM synchronous motor and the CPPM hybrid excitation synchronous motor is changed stator magnetic ring with the excitation winding, shown in Fig. 1(b) and Fig. 1(c).

2.2 Mathematical model of the CPPM machine

The radial flux component produced by stator permanent magnet ring in CPPM machine is similar with that produced by rotor excitation winding in a wound excitation synchronous machine. The stator permanent magnet ring excitation flux and rotor permanent magnet flux will combine in the airgap region. Therefore, the flux linkage of the CPPM machine can be described by the following equation:

$$\begin{bmatrix} \psi_d \\ \psi_q \end{bmatrix} = \begin{bmatrix} L_d & 0 \\ 0 & L_d \end{bmatrix} \begin{bmatrix} i_d \\ i_q \end{bmatrix} + \begin{bmatrix} \psi_{r-pm} + \psi_{s-pm} \\ 0 \end{bmatrix} \quad (1)$$

Where the ψ_{r-pm} is rotor permanent magnet flux, ψ_{s-pm} is stator ring permanent magnet flux. The electromagnetic torque can be expressed as follows:

$$T_e = 1.5P[(\psi_{r-pm} + \psi_{s-pm})i_q + (L_d - L_q)i_d i_q] \quad (2)$$

2.3 Magnetic adjustment principle

When the CPPM synchronous motor running under the no-load conditions, due to the high magnetic resistance of the rare earth permanent magnet in the rotor, most of the magnetic flux generated by the stator ring operates along the iron pole of the left and right rotor parts, and is closed by the axial magnetic circuit. At this time, the polarity of the iron pole is the same as the polarity of the permanent pole on the other side. The magnetic flux path is shown in Fig. 2(a) and (b). When the armature winding enters the direct axis demagnetization current, most of the armature reaction flux goes around the two section rotor iron pole from right side to the left side, and closes through the radial magnetic circuit. As shown in Fig. 3(a), the armature reaction flux at the iron pole is opposite to that of the magnetic ring in Fig. 2(b). The synthetic flux of the iron

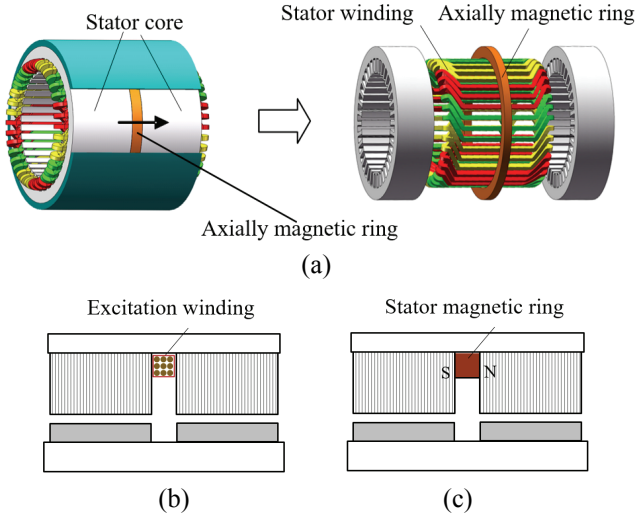

Fig. 1. Stator structure comparison of the CPPM synchronous motor and the CPPM hybrid excitation synchronous motor: (a) 3-D view of the CPPM synchronous motor stator; (b) 2-D view of the CPPM synchronous motor; (c) 2-D view of the CPPM hybrid excitation synchronous motor

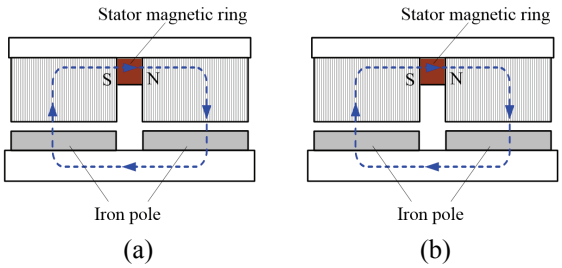

Fig. 2. Magnetic flux path generated by the stator magnetic ring of the CPPM synchronous motor: (a) 2-D plane graph, (b) 3-D sketch map

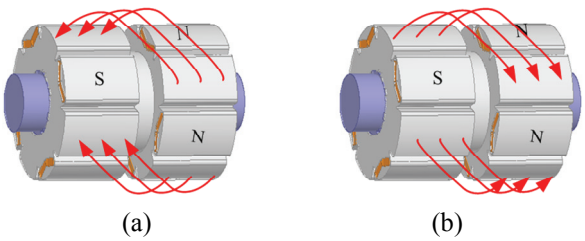

Fig. 3. Rotor flux path under the armature reaction: (a) Case of demagnetization. (b) Case of magnetization

pole decreases and plays the demagnetizing effect. When the armature winding enters the direct axis magnetization current, most of the armature reaction flux goes around the two section rotor iron pole from left side to the right side, and closes through the radial magnetic circuit. As shown in Fig. 3(b), the armature reaction flux at the iron pole is same to that of the magnetic ring in Fig. 2(b). The synthetic flux of the iron pole increases and plays the magnetizing effect.

Fig. 4 is the 3-D finite element analysis and Fourier analysis result of the air gap magnetic field when the CPPM synchronous motor is running under the no-load condition (synthesis excitation of the stator and rotor permanent magnets). The magnetic flux generated by the permanent magnetic ring forms a loop through the rotor iron pole. The magnetic flux density of the air gap in the iron region is 0.87T. Fig. 5 shows the results of three-dimensional finite element simulation and Fourier analysis of air gap magnetic field when the CPPM synchronous motor armature winding passes through a small straight-axis demagnetizing current (138 AT). The magnetic flux density of the air gap in the iron region is 0.70T. The air gap flux density in the iron pole region is reduced by 20% while the magnetic flux density of the permanent magnetic pole region is almost constant. It shows that CPPM synchronous motor has good magnetic weakening capability.

3. Comparative Analysis

3.1 Permanent magnet synchronous motor

Same as permanent magnet synchronous motor, the CPPM synchronous motor also realizes weakening or increasing magnetism by controlling the armature current. However, the permanent magnet synchronous motor has large direct axis reluctance, a large armature current is required to increase the speed in flux weakening region. This will lead to an increase in copper loss, especially the air gap magnetic field waveform will be deterioration, and a larger iron loss produced in high-speed case will reduce motor efficiency, increase the temperature rise of the motor [14].

Fig. 6 is the air gap flux density waveform and spectrum analysis result of the Toyota Prius permanent magnet synchronous motor (hereinafter referred to as Prius motor)

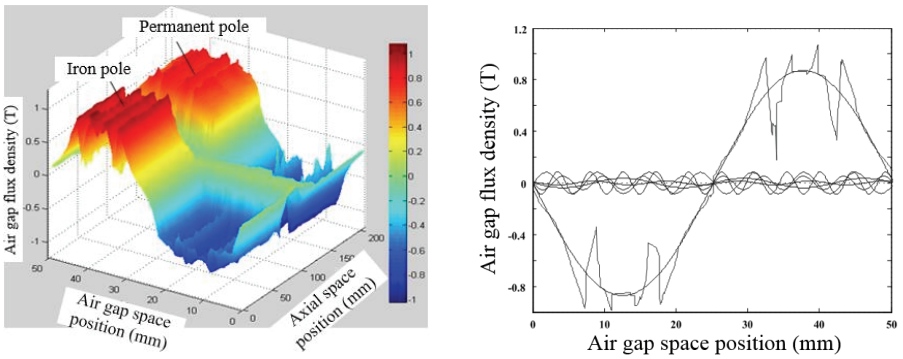

(a) (b)

Fig. 4. Air gap flux density of the CPPM synchronous motor under the no-load condition: (a) 3-D finite element analysis. (b) Fourier analysis result

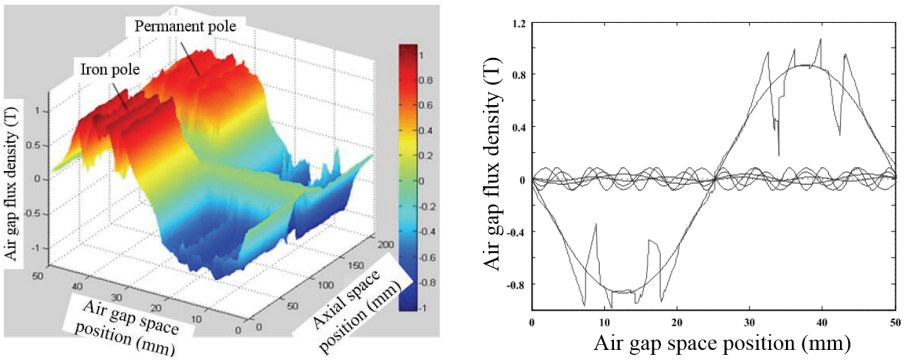

(a) (b)

Fig. 5. Air gap flux density of the CPPM synchronous motor under the demagnetization case: (a) 3-D finite element analysis, (b) Fourier analysis result

when the armature winding passes through the 77 A direct axis weak magnetic current. No-load air gap fundamental magnetic density of the Prius motor is about 0.73 T, demagnetizing ratio is 55%. The 5th harmonic amplitude is 0.43 T which is 0.1T higher than higher than that of the fundamental magnetic density, and the distortion rate of the air gap flux density is 158%. As the 5th and 7th harmonic magnetic flux is large, the stator iron loss of Prius motor is higher at high speed region, and the core temperature rise is higher. Iron loss analysis of the Prius motor under the 6000 r/min and the direct axis demagnetization current of 77 A conditions is shown in Fig. 7(a), and the average iron loss is 1090 W. By adjusting the parameters of the Prius motor's permanent magnet, the fundamental air gap magnetic flux density of the Prius motor model is 0.33 T, the iron loss analysis under the 6000 r/min is shown in Fig. 7 (b), and the average iron loss is 77 W.

The speed range of permanent magnet synchronous motor used in pure electric vehicle drive is higher than that of hybrid motor vehicle. Larger direct axis current is required to realize the flux weakening regulation, air gap magnetic field waveforms will be worse and the armature winding copper loss and stator core loss will be greater. Meanwhile, the permanent magnetic pole will also face greater demagnetization risk.

Unlike the permanent magnet synchronous motors, straight axis armature flux of the CPPM Synchronous Motor does not pass through the high reluctance of the rare earth permanent poles, a closed magnetic circuit is formed through the rotor iron pole. The direct axis magnetic circuit has small magnetic resistance and direct axis armature current has strong magnetic modulation ability but little influence on the air gap magnetic field waveform. There is no risk of demagnetization in the permanent magnet.

3.2 CPPM hybrid excitation synchronous motor

The magnetic field analysis of CPPM hybrid excitation synchronous motor under the demagnetization case is shown in Fig. 8, where F_δ is the air gap synthesis magnetomotive force, F_{pm} is the rotor permanent magnet magnetomotive force and the F_l *is the* magnetomotive force obtained from the stator magnetic ring. It can be seen from Fig. 8 (a) that the axial component of the air gap synthesis magnetomotive force is large and the tangential component is small when the motor is running under the flux weakening speed control conditions, So that the middle part of the magnetic shell appears severe saturation is shown in Fig. 8(b). The flux linkage of the CPPM hybrid excitation synchronous motor has been

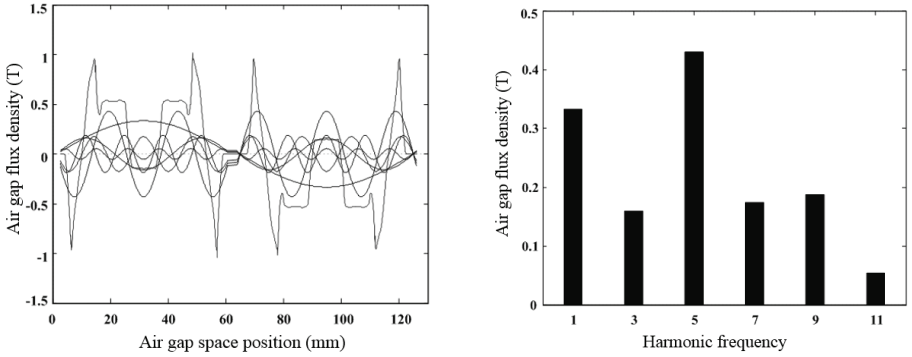

(a) (b)

Fig. 6. Air gap flux density waveform and spectrum analysis of the Prius motor: (a) Fourier analysis result; (b) Spectrum analysis result

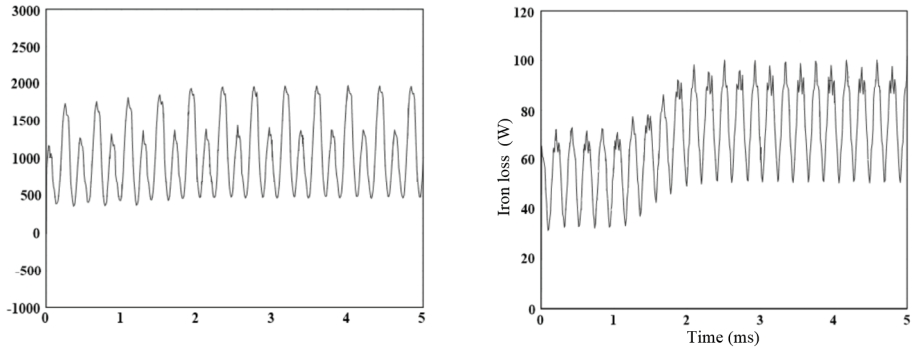

(a) (b)

Fig. 7. Iron loss analysis of the Prius motor under the 6000 r/min: (a) Original iron loss; (b) Iron loss after the permanent magnet adjustment

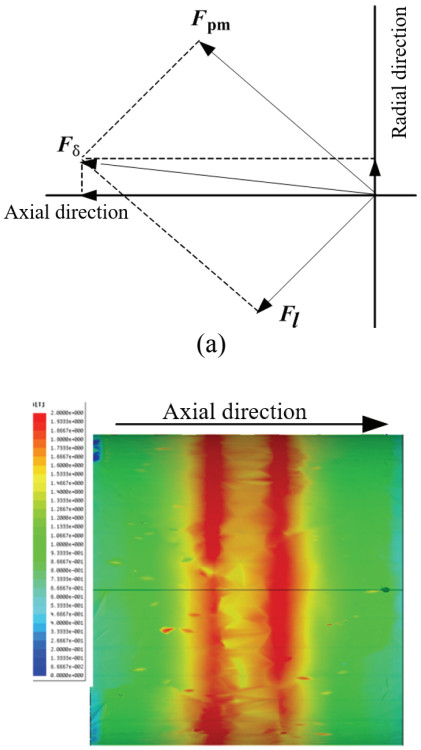

Fig. 8. Magnetic field analysis of CPPM hybrid excitation synchronous motor under the demagnetization case: (a) Magnetomotive vector; (b) Axial magnetic density map

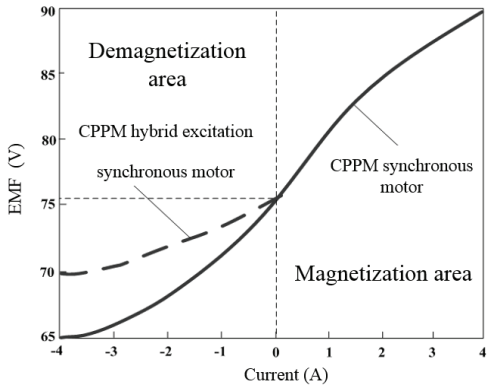

Fig. 9. CPPM machine's EMF vs. armature characteristics

defined in [15].

Analytical curves of induction electromotive force generated by armature winding with different armature currents in CPPM synchronous motor are shown in Fig. 9 [9]. It can be seen from the figure, the induced electromotive force increases by about 14V when the magnetizing current is increased by 4A, while the 4A demagnetization current induced electromotive force reduced by about 11V in CPPM synchronous motor. It is found that the difference induced electromotive force under the same magnetizing and demagnetizing current amplitude is about 3V. It shows that CPPM synchronous motor has little difference during the increasing magnetic flux and weakening magnetic flux processing. On the other hand, comparing the dashed lines in the graph, it can be found that the induction electromotive force difference between the CPPM hybrid excitation synchronous motor and the CPPM synchronous motor is 5V under the same 4A demagnetization current. This difference can be interpreted as the magnetic flux runs along the radial magnetic circuit in CPPM synchronous motor under flux weakening condition, there is no saturation problem of the axial magnetic circuit, which improves the wide range magnetic flux weakening capability of the motor.

Compared with CPPM hybrid excitation synchronous motor, the main advantages of CPPM synchronous motor can be summarized as follows:

(1) Using axial permanent magnetic ring excitation instead of current excitation of CPPM hybrid excitation synchronous motor, the motor manufacturing process is simplified, the excitation loss is eliminated, and the motor efficiency is further improved.

(2) The rotor pole of the CPPM hybrid field synchronous motor is retained, the magnetic resistance of the direct axis magnetic circuit is small. It overcomes the disadvantage that the axial magnetic circuit is saturated and the magnetic field is narrow when the CPPM hybrid excitation synchronous motor is running under the flux weakening conditions.

(3) Eliminating the CPPM hybrid excitation synchronous motor magnetic shell and DC excitation power supply, the volume and weight of the motor and the controller are saved, and the manufacturing cost of the system is reduced.

As an electric vehicle drive motor, When the CPPM synchronous motor is running in the constant torque zone, the permanent magnetic ring generates magnetic flux through the iron pole, the id = 0 control strategy can be adopted to improve the electromagnetic torque of the motor. In the constant power region operation region, the armature current of the straight shaft plays a role in demagnetizing on the iron field, to achieve flux weakening speed rise. Therefore, CPPM synchronous motor takes into account both flux weakening and torque requirements, with good traction characteristics.

4. Prototype and Experiment

In order to verify the aforementioned principles and characteristics of the CPPM synchronous motor, a 750W CPPM synchronous motor is designed, fabricated and tested. 750W CPPM synchronous motor prototype and rotor part are shown in Fig. 10 and Fig. 11. Table 1 shows the main design parameters and electrical specifications of the prototype. The no-load electromotive force and the Fourier analysis waveform are shown in Fig. 12.

Table 1. Main parameters and electrical specifications of the prototype

Design Parameters	Values (unit)
Rated power	750 (W)
Rated voltage	220 (V)
Rated speed	1500 (r/min)
Pole & slot	8/24
Stator core outside / inside diameter	110/65 (mm)
Stator core length	85 (mm)
Magnetic ring outside / inside diameter	110/90 (mm)
Magnetic ring magnetization direction thickness (axial direction)	3.5 mm

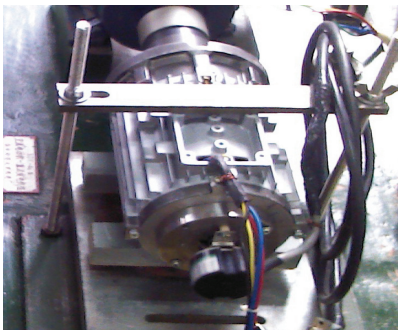

Fig. 10. 750W CPPM synchronous motor prototype

Fig. 11. Rotor part of the prototype

4.1 Flux weakening experiment

The purpose of the flux weakening experiment is to verify the weak magnetic adjustment capability of the CPPM synchronous motor and whether there has a local saturation problem in the axial magnetic circuit. In the experiment, the CPPM synchronous motor keeps the speed at the 500 r/min with no-load operation condition. At this point, the q axis current is small, the effect of the q axis current act on the d axis current can be neglected. The relationship between the d axis current and the no-load EMF is shown in Fig. 13. When the CPPM synchronous motor armature winding is injected with 3.9 A d-axis magnetizing current, The EMF increases from 70.8 V to 83.1 V. When the CPPM synchronous motor armature winding is injected with 3.9 A d-axis demagnetizing current, The EMF decreases from 70.8 V to 47.1 V. It shows that the CPPM synchronous motor has good magnetic flux regulation ability. Moreover, there is no local saturation phenomenon when the CPPM synchronous motor is running under the flux weakening field.

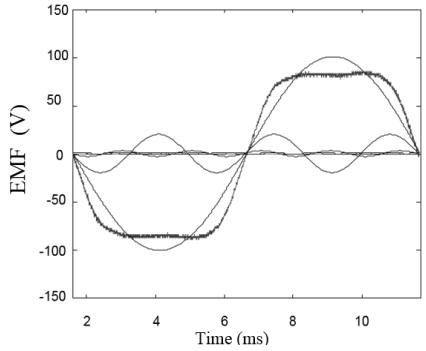

Fig. 12. No-load electromotive force and the Fourier analysis waveform of the prototype

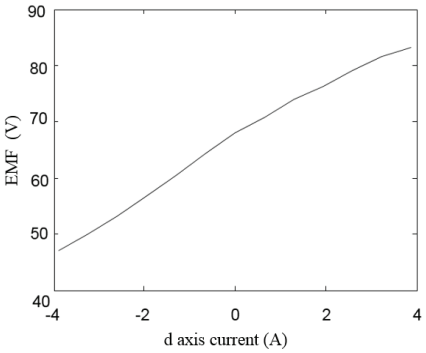

Fig. 13. Relationship between the d axis current and the no-load EMF

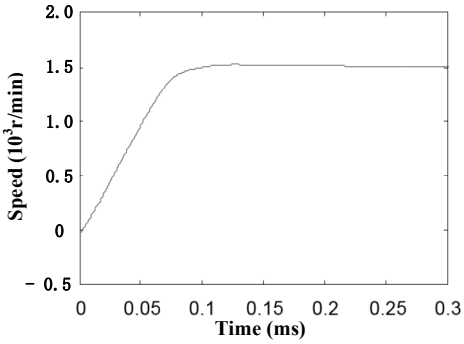

Fig. 14. Speed response curve of the CPPM synchronous motor prototype under the no-load starting condition

4.2 Starting experiment

Fig. 14 shows the speed response curve of the CPPM synchronous motor prototype under the no-load starting condition, with a motor speed of 1500 r/min. From the figure we can see that the linear start characteristics can be achieved by the prototype. Fig. 15 shows the q-axis current response curve when the prototype is started, peak q-axis current at start-up does not exceed 7A and after entering the steady state, the q axis current is about 0.5A.

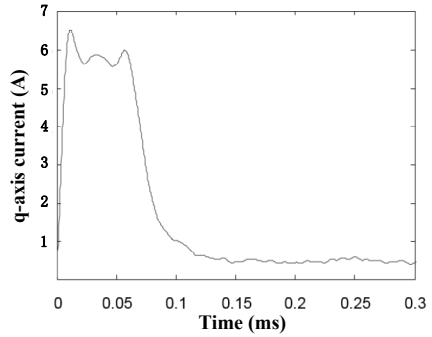

Fig. 15. q-axis current response curve of the prototype

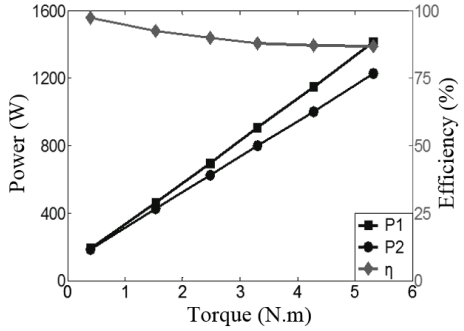

Fig. 16. Load characteristic curve when the prototype is running at 2000 r/min

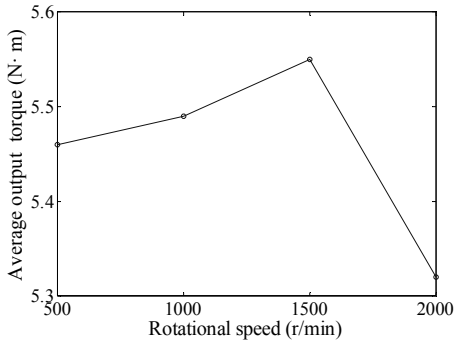

Fig. 17. Average output torque versus speed of the prototype

4.3 Test results for load characteristics

In the load test, the speed of the CPPM synchronous motor is given by the controller. Hysteresis dynamometer is used to regulate the prototype load. The relationship between the input power P1, motor output power P2, efficiency η and the motor output torque is shown in Fig. 16 when the prototype is running at 1500 r/min. The efficiency results show that the prototype has the high efficiency in light load, and the efficiency at rated load is about 87%. Variation of the measured average output torque with speed is shown in Fig. 17. The prototype operates primarily in the constant torque region from the 500r/min to the 2000r/min.

5. Conclusion

A novel CPPM synchronous motor suitable for the new energy vehicle applications was proposed and investigated. The proposed machine overcomes the shortcomings of the traditional permanent magnet synchronous motor and CPPM hybrid excitation synchronous motor. As a new type of permanent magnet synchronous motor, thanks to the permanent magnet magnetic ring on the stator side of the CPPM synchronous motor and the iron pole structure on the rotor, it has a wide range of field weakening capability and high operating efficiency. Compared with the magnetization field of the CPPM synchronous motor, the change of the EMF is about 2 times of the flux weakening field. The experimental results show that the CPPM synchronous motor has strong magnetic flux weakening ability, and solves the problem of local saturation of the axial magnetic circuit when the machine is running under the flux region field.

Acknowledgements

This work was supported by a grant from National Natural Science Foundation of China (NSFC) under Project No. 61501419.

References

[1] Burress T A, Coomer C L, Campbell S L, et al. Evaluation of the 2007 Toyota Camry Hybrid Syneregy Drive System[J]. Fuel Efficiency, 2008.

[2] Goss, M. Popescu, D. Staton, R. Wrobel, J. Yon and P. Mellor, "A comparison between maximum torque/ ampere and maximum efficiency control strategies in IPM synchronous machines," *2014 IEEE Energy Conversion Congress and Exposition* (*ECCE*), Pittsburgh, PA, pp. 2403-2410, 2014.

[3] Burress T A, Campbell S L, Coomer C, et al. Evaluation of the 2010 Toyota Prius Hybrid Synergy Drive System[J]. Office of Scientific & Technical Information Technical Reports, 2011.

[4] S. Yoshioka, S. Morimoto, M. Sanada and Y. Inoue, "Influence of magnet arrangement on the performance of IPMSMs for automotive applications," *2014 IEEE Energy Conversion Congress and Exposition (ECCE)*, Pittsburgh, PA, pp. 4507-4512, 2014.

[5] Tapia J A, Leonardi F, Lipo T A. Consequent pole permanent magnet machine with field weakening capability[C]// Electric Machines and Drives Conference, 2001. IEMDC 2001. IEEE International. IEEE, 2001:126-131.

[6] Y. Liu, Z. Zhang and X. Zhang, "Investigation of

hybrid excitation synchronous machines with built-in field windings," *2016 XXII International Conference on Electrical Machines (ICEM)*, Lausanne, pp. 2544-2550, 2016.
[7] Xiao-yong Zhu, Ming Cheng, Wen-xiang Zhao. An overview of hybrid excited electric machine capable of field control [J]. Transactions of China Electro-technical Society, vol. 23, no. 1, pp. 30-39, 2008.
[8] H. J. Kim, D. Y. Kim, J. S. Jeong and J. P. Hong, "Proposition of Structures for Brushless Hybrid-Excitation Synchronous Motors With Improved Rotor," *in IEEE Transactions on Magnetics*, vol. 52, no. 9, pp. 1-15, Sept. 2016.
[9] Z. Zhang, Y. Liu, B. Tian and W. Wang, "Investigation and implementation of a new hybrid excitation synchronous machine drive system," in *IET Electric Power Applications*, vol. 11, no. 4, pp. 487-494, 2017.
[10] M. Aydin, S. R. Huang , T. A. Lipo. A new axial flux surface mounted permanent magnet machine capable of field control[C]. *IEEE Industry Applications Society Annual Meeting*, 2002:1250-1257.
[11] Juan Tapia. Development of the consequent pole permanent magnet machine. A thesis of Ph.D. at University of Wisconsin-madison. 2002.
[12] Xinhua Li, Minhua Wu, Gaoxiong Liu, Ping Weng. Finite ElementAnalysis ofM agnetic Field for CPPM Hybrid-ExcitationW ind-Turbine Generators [J]. Small & Special Electrical Machines, 2011, 39(5): 5-7.
[13] Xiaojiang Wu . Study on CPPM double-permanent synchronous motor in electric vehicle [D]. A thesis of master's degree at Hubei University of Technology , 2013.
[14] Zhang B, Qu R, Wang J, et al. Thermal Model of Totally Enclosed Water-Cooled Permanent-Magnet Synchronous Machines for Electric Vehicle Application[J]. *IEEE Transactions on Industry Applications*, vol. 51, no. 4, pp. 3020-3029, 2014.
[15] Zheran Li, Yesong Li, Xinhua Li. Flux Control of a CPPM Machine for Both a Wide Speed Range and High Efficiency[J]. *IEEE Transactions on Power Electronics*, vol. 29, no. 9, pp. 4866-4876, 2014.

Kun Xie is a Ph.D. student in the State Key Laboratory of Ocean Engineering at Shanghai Jiao Tong University, Shanghai, China. He received his B.S. (2008) and M.S.(2011) in mechanical engineering from Zhejiang University, Hangzhou, China. His core research interests include ship energy saving and electrical engineering. He is currently working on electrical engineering and ship energy saving.

Xinhua Li was born in Hubei Province, China, in 1959. He received the B.E. degree from the School of Electrical and Electronic Engineering, Huazhong University of Science and Technology, Wuhan, China, in 1982. From 1990 to 1991, he was a Visiting Scholar with the School of Electrical and Electronic Engineering, Huazhong University of Science and Technology, Wuhan, China. Since 2001, he has been a Full Professor in the School of Electrical and Electronic Engineering, Hubei University of Technology. From 2002 to 2004, he was an Adjunct Professor with the Electric Vehicle Research Institute, Huazhong University of Science and Technology, Wuhan, China. His current major research interests include the design and control of novel permanent-magnet machines for automotive applications.

Jimin Ma was born in China. He received the B.E.E. and M.S.E.E. degrees from Wuhan University of Technology, Wuhan, China, in 2002 and 2006, respectively, and the Ph.D. degree in electrical engineering from Huazhong University of Science and Technology, Wuhan, China, in 2017. His main research interests include design and control of reluctance machines, novel permanent-magnet brushless machines.

Xiaojiang Wu was born in Jiangxi Province, China in 1986. He received the M.E. degree from the School of Electrical and Electronic Engineering, Hubei University of Technology, Wuhan, China, in 2013. His current major research interests include the electromagnetic and structure design of BLDC for UAV.

Hong Yi is a Professor in the State Key Laboratory of Ocean Engineering at Shanghai Jiao Tong University, Shanghai, China. He received his Ph.D. degree in 2002 from Shanghai Jiao Tong University. He has been teaching at Shanghai Jiao Tong University since 1991. His core research interests include virtual reality technology and ship reliability engineering. He is currently working on virtual reality technology and ship reliability engineering.

Gangyi Hu is a Professor in China Ship Development and Design Center, Wuhan, Hubei, China. He received his Ph.D. degree in 2011 from China Ship Research and Development Academy. He has been developing several different types of ship since 1991. His core research interests include automation technology and ship development engineering. He is currently working on automation technology and ship development engineering.